

Fujitsu Quantum Simulator Challenge 2023 Report: **Quantum Machine Learning Applied to Alzheimer's Disease Diagnosis and Management**

Ramachandran Sekanipuram Srikanthan and Eric Rotenberg
Department of Electrical and Computer Engineering
North Carolina State University
Raleigh, North Carolina, 27695, USA

1. Introduction

Alzheimer's disease (AD) is a subset of dementia caused by the accumulation of plaques in between the neural connections of the brain. These plaques prevent the transmission of neural signals between different neurons, thereby removing their connections and causing memory loss.

Our project applies Quantum Computing, and specifically Quantum Machine Learning (QML), to three aspects of AD intervention. The three aspects are summarized below and elaborated in the three technical sections of this report.

1. Section 2: Detect AD in its early stages from structural MRI images of the brain. Methodology used for this part: we explored various *hybrid classical-quantum ML models* using the Google Collab cloud computing service.
2. Section 3: Identify drugs that target and slow down the impact of AD. Methodology used for this part: we explored *quantum ML circuits* using the **Fujitsu Quantum Simulator**.
3. Section 4: Discover new drugs for AD using Quantum Generative Adversarial Networks (Quantum GANs). Methodology used for this part: we explored *quantum ML circuits* using the **Fujitsu Quantum Simulator**.

Please note, as highlighted above, that the Fujitsu Quantum Simulator was used only in Sections 3 and 4. The reasons we included Section 2 in this report (though not based on Fujitsu's simulator) are two-fold: (1) to provide complete context for our overall project; (2) to give experimental evidence of our main hypothesis in the Fujitsu Quantum Simulator Challenge:

Hypothesis (and motivation for using Fujitsu's parallel quantum simulator): There may be two ways to increase QML accuracy: (1) increase the parameterized quantum circuit depth (ansatz depth) which, in turn, increases the number of tunable parameters; (2) increase the number of qubits, hence, increase the state space. Our hypothesis is that the latter is superior, *i.e., the Fujitsu-enabled huge state space is more effective at increasing QML accuracy than increasing tunable quantum circuit parameters*. This is not only our hypothesis but also a key motivation for participating in the Fujitsu Quantum Simulator Challenge, because Fujitsu's simulator can parallelize the simulation of the huge state space and makes it computationally feasible.

In Sections 3 and 4, we describe challenges we faced scaling the number of qubits for our quantum ML circuits on Fujitsu's quantum simulator. In a final section, Section 5, we address each of the evaluation criteria for the Fujitsu Quantum Simulator Challenge.

2. Classification of MRI brain images

We use the structural MRI scan images of the brain provided by Kaggle's open source dataset and train a computation model to predict the stage of dementia. The model categorizes these structural MRI into a very mildly demented, mildly demented, or moderately demented stage based on the severity.

2.1 Data preprocessing

The project utilizes Kaggle's open source dataset for training the computational model. The open source dataset from Kaggle [4] contains hand collected images from various websites with each label verified. It contains separate train and test datasets with a total of 6400 image samples each of which is categorized as mildly demented, very mildly demented, moderately demented and non-demented.

2.2 Hybrid classical-quantum ML model

We will be using various Classical Deep learning techniques along with Quantum Computation to formulate the model required to produce the desired prediction. The models which are being used are described in the section below.

2.2.1 Deep Residual learning - Resnet34

These kinds of classical models use Deep learning techniques to train and perform inference on the dataset. The main advantage of using Deep Residual learning [7] comes from its architecture.

Previously, as the depth of the neural network increases to obtain more trainable parameters, the gradient propagation from the final layer to the initial layer either vanishes causing a vanishing gradient problem or explodes causing an exploding gradient problem. To overcome this issue, Deep Residual networks come into play.

Deep Residual networks contain various skip connections between the neural network layers. The skip connections in the architecture are denoted by the below figure.

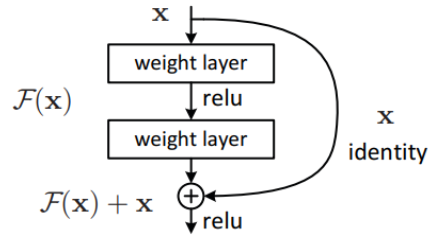


Figure 1 - Deep residual network

During forward propagation, it moves through all the layers without skipping and produces the prediction. But during backpropagation, the gradients flow through the skip connections and thereby avoiding vanishing and exploding gradient problems while training.

2.2.2. Hybrid Quantum Classical Machine learning model

Classical models which use deep learning techniques are proven to be good feature extractors for the provided data. These models can be trained using various optimization techniques to extract the best features from the input data for which the prediction is being generated. On the other hand, quantum computing enables us to tap into the higher dimensional Hilbert space using various gate operations. By combining both the techniques, we can gain a lot of advantages in modeling.

The figure 2 below shows the architecture of the hybrid quantum classical model. The resnet34 classical model acts as a feature extractor for the dataset. The final 512 neurons from this resnet34 is being downsized to the number of qubits being used in the quantum model. The measurement output from the quantum model is again passed to linear neurons based on the number of output classes.

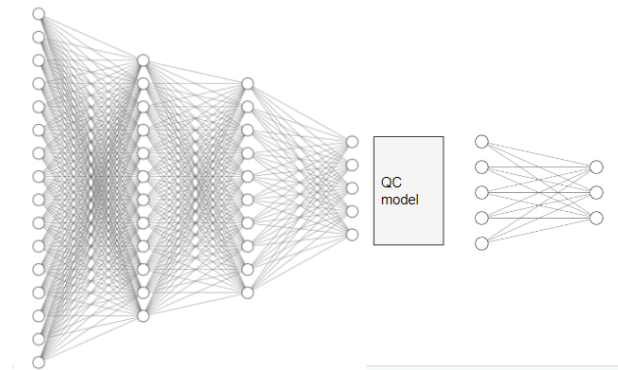


Figure 2 - hybrid quantum classical model architecture

The figure 3 below shows the architecture of the quantum model [8] being used. The quantum model architecture comprises 4 sections - initial state preparation, transformation, trainable ansatz and measurement.

- *Initial State preparation* - In this stage, the initial qubit state is being prepared. It can be in all 0 states or it can be in superposition of all the 2^n states for n-qubit circuits.
- *Transformation* - In this stage, the classical data is being transformed into the hilbert space. In this hybrid architecture, we use angle embedding to achieve this. The classical data from the Resnet34 is being taken as the angle of rotation within the Hilbert space. The embedding can be done by either X, Y or Z rotation in the Hilbert space.
- *Trainable Ansatz* - Here, we perform the training operation. The Ansatz contains a set of gates along with linear entanglement. The angles of these gates are being optimized to converge into the final solution.
- *Measurement* - This is the final stage of the model where we convert the data from the hilbert space to the classical world.

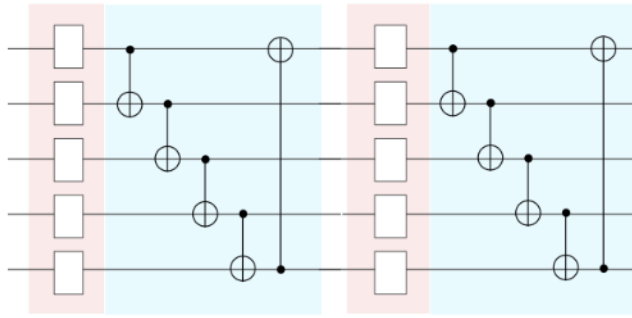


Figure 3 - Quantum model architecture

In our analysis, we will be using Resnet34 as the classical feature extractor model and quantum model with the below specifications as the trainable classifier.

- *Initial State preparation* - Superposition of all possible states.
- *Transformation* - Angle Embedding (Y rotations).
- *Trainable Ansatz* - Basic Entangler Ansatz (trainable Y rotation with CNOT entangler between each qubit and qubit+1).
- *Measurement* - Z measurement in all qubits.

To prove our hypothesis, we will be varying the number of qubits and the ansatz repetition depth of the Quantum model.

2.3 Simulator used

The model training and the evaluation code is being developed using Python along with the Pytorch [29] and PennyLane [8] packages. It's been developed on a Google Colaboratory based Jupyter notebook and has been run on Google Cloud Instance with T4 GPU and CUDA enabled.

2.4 Results

The dataset contains the pre-processed structural MRI scans of various patients being

labeled based on their class. We use this dataset to train a model which can early detect the stage of dementia for newer patients. The hyperparameters used are mentioned below.

- Batch Size - 8
- Learning Rate - 1E-5
- Epochs - 25
- Loss (Cost) Function - Cross Entropy
- Optimizer - Adam

The results of training the model have been summarized in the below table. It can be seen that hybrid quantum classical models have better accuracy than their corresponding classical model. This shows the advantage of using quantum computing along with classical deep learning techniques.

Model	Accuracy (%)
Resnet34 (Classical)	95.46%
Resnet34 + QML Qubits - 4 Depth - 1	96.09%
Resnet34 + QML Qubits - 4 Depth - 2	95.70%
Resnet34 + QML Qubits - 4 Depth - 4	97.57%
Resnet34 + QML Qubits - 8 Depth - 1	96.015625%
Resnet34 + QML Qubits - 8 Depth - 2	96.953125%
Resnet34 + QML Qubits - 8 Depth - 4	96.484375%
Resnet34 + QML Qubits - 16 Depth - 1	97.5%

The depth (ansatz repetition depth) vs length (# qubits) graph of the hybrid quantum classical model has been shown in Figure 4. The classical model (Resnet34) acts as the feature extractors for the dataset. It can be seen that the quantum model which uses 8 qubit and ansatz repetition depth 1 converges better and faster compared to the quantum model with 4 qubits and ansatz repetition depth 2 with both having the same number of trainable parameters in their ansatz (8 parameters).

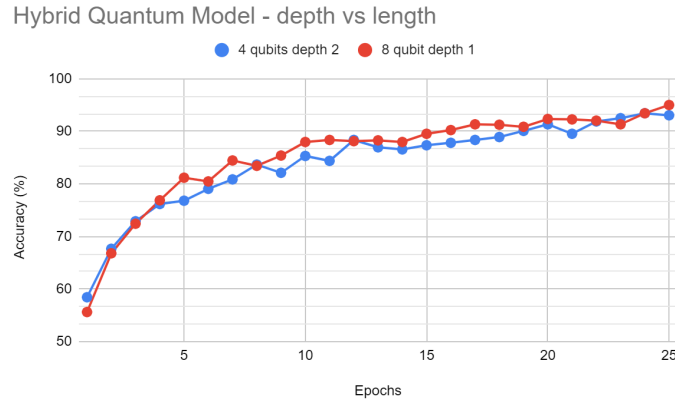


Figure 4 - Depth vs Length graph 1

A similar trend can also be shown in Figure 5. The classical model (Resnet34) acts as the feature extractors for the dataset. It can be seen that the quantum model which uses 16 qubits and ansatz repetition depth 2 converges better and faster compared to the quantum model with 8 qubits and ansatz repetition depth 4 with both having the same number of trainable parameters in their ansatz (32 parameters).

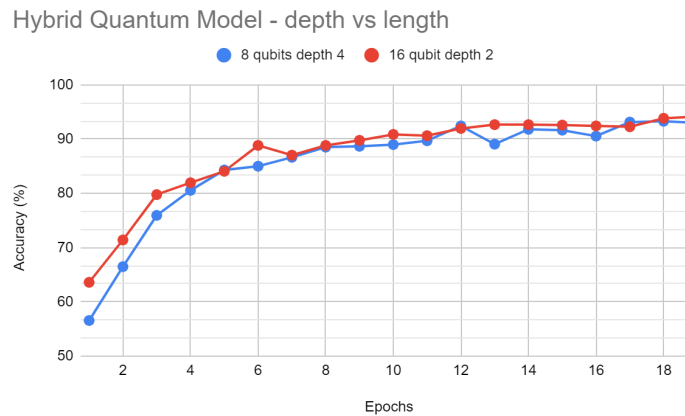


Figure 5 - Depth vs Length graph 2

We can further prove the case with a higher number of qubits based on the plot in Figure 6. It can be seen that the quantum model which uses 16 qubits and has an ansatz repetition depth 1 outperforms the quantum model with 8 qubits and ansatz repetition depth of 2. The 16

qubit with ansatz repetition depth 1 model also outperformed the 4 qubit ansatz repetition depth 4 model. All the models have the same number of trainable parameters in their ansatz (16 parameters).

It can also be seen that the quantum model with 8 qubits and ansatz repetition depth 2 does not outperform the quantum model with 4 qubits and ansatz repetition depth 4. This is due to the Barren plateau problem. The quantum models with more qubits are more susceptible compared to quantum models with less qubits to this barren plateau issue. Thus increasing the ansatz repetition depth to 2 in a 8 qubit system suffers more plateauing than having an ansatz repetition depth to 4 in a 4 qubit system.

Thus, the above data supports our Hypothesis, that a Fujitsu-enabled huge state space (many qubits) may be more effective at increasing QML accuracy than increasing tunable quantum circuit parameters (deeper parameterized quantum circuit).

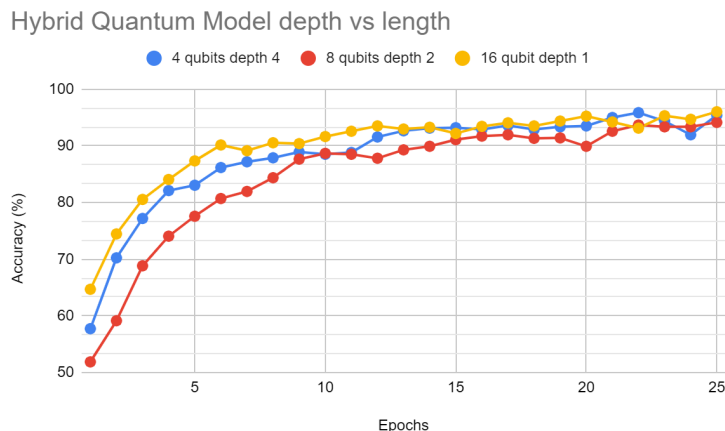


Figure 6 - Depth vs Length graph 3

3. AD drug identification

Here, we find out the drug targets which have potential bioactivity towards reducing the progression of this disease. Using an open source dataset from ChEMBL, a computational model is trained to predict the possible drug compounds which slow down the progression. A suitable generative model is also trained to create newer drug structures targeting the disease.

(AChe) [17] inhibitors are effective in slowing down (or reversing) Alzheimer's disease and Myasthenia gravis. Alzheimer's Disease is characterized by lower levels of Acetylcholine than normal cognition. Acetylcholine is a neurotransmitter that breaks down into acetate and choline. Its role is to terminate neuronal transmission and signaling between synapses.

Acetylcholinesterase (AChE) inhibitors result in higher concentrations of acetylcholine and better communication between neurons. This can temporarily improve or stabilize Alzheimer's disease symptoms. Current AChE inhibitor treatments available for AD include Donepezil, galantamine and Rivastigmine.

The dataset is taken from an open source database [5] (ChEMBL) containing the drugs and their corresponding targets. The dataset contains 4620 samples of drug molecules which target Alzheimer's disease.

3.1 Data preprocessing

The database is queried for single protein targets based on their bioactivity towards inhibiting this AChE inhibitor. The bioactivity data for Human Acetylcholinesterase which has target values has been selected for model training. The main parameter used here for training the model is the IC50 value.

Half maximal inhibitory concentration (IC50) is a measure of the potency of a substance in inhibiting a specific biological or biochemical function. IC50 is a quantitative measure that indicates how much of a particular inhibitory substance (e.g. drug) is needed to inhibit, in vitro, a given biological process or biological component by 50%. Lower the number of IC50, the better the potency of the drug becomes. IC50 is represented using molar concentration.

The bioactivity data is the IC50 value. Compounds having values of less than 1000 nM will be considered to be active while those greater than 10,000 nM will be considered to be inactive. As for those values between 1,000 and 10,000 nM will be referred to as intermediate. The dataset is prepared [15] with the molecular ID, the Canonical SMILES representation of the molecule and their corresponding IC50 value.

The dataset contains the corresponding molecular features and their bioactivity class. At first, the low variance features are being removed for each molecule and therefore we will be left with 140 features in total. It's been divided into train and test sets with each being 80% and 20% respectively.

3.2 Quantum circuit

The project uses a pure Quantum Machine learning model for performing the training and inference. The molecular feature data with 140 elements are being grouped together into groups of 14 features and converted into a decimal representation. This creates a dataset with 10 decimal values for each molecule which is used for training and inference. We create a quantum model with 10 qubits based on the below specifications.

- *Initial State preparation* - Superposition of all possible states.
- *Transformation* - Angle Embedding (Y rotations).

- *Trainable Ansatz* - Strongly Entangled Ansatz as described in Figure 7. Finally, we add a set of CNOT entanglers between each qubit with the first qubit having the first qubit as target.
- *Measurement* - Z measurement in the first qubit scaled by 2 (range between -1 and 1).

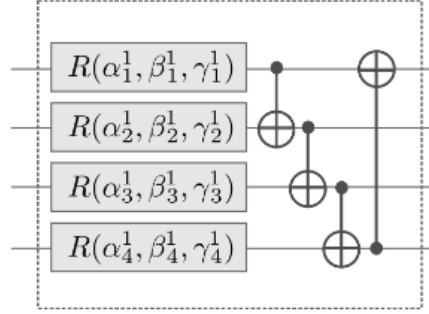


Figure 7 - Strongly Entangled Ansatz

3.3 Simulator used

This is being coded with Python and using the mpiQulacs package provided by the Fujitsu environment. It is run on a Fujitsu cluster simulator as described in reference paper [21].

3.4 Results and challenges

The hyperparameters of the model are described below.

- Max iterations - 700
- Batch Size - 1
- Loss function - Cross entropy loss
- Optimizer - L-BFGS-B

3.4.1 Gradient estimation challenges

The output of the variational circuit is the expectation value of a measurement observable, which can be formally written as a parameterized “quantum function” $f(\theta)$ in the tunable parameters $\theta = \theta_1, \theta_2, \dots$. The quantum gradient is obtained by computing the partial derivatives of function f with respect to its parameters.

$$\nabla_{\theta} f(\theta) = \left(\partial_{\theta_1} f \ \partial_{\theta_2} f \vdots \right)$$

The gradients are estimated using the parameters shift rule as described in reference paper [24]. The Numerical differentiation [24] approach for computing the gradient involves shifting the quantum circuit’s parameters by small values and finding the change in the output.

$$\nabla g(x) \approx (g(x + \Delta x/2) - g(x - \Delta x/2))/\Delta x, \quad (2) \text{ where } \Delta x \text{ is a small shift}$$

This is then followed by using gradient descent optimization algorithm to find out the minimum optimal value for a given cost function.

Currently, Qulacs [28] library does not support this gradient computation using the parameter shift approach for each iteration of model training. Due to this limitation, Gradient based optimizers such as Stochastic gradient descent cannot be used for training the quantum model.

Thus, the quantum model is trained using Quasi-Newton methods, which approximate the Hessian (or finite differences of gradients). Thus, these Quasi-Newton methods limit the training capability of the quantum model.

3.4.2 Results with 10 qubits one node

The pure quantum model is being trained using the above hyperparameters using 10 qubits and an ansatz repetition depth of 4. The model is trained using a single node from the Fujitsu simulation cluster and an accuracy of 57.35% is reached.

3.4.3 Problems with 20 qubits one node

When the pure quantum model is trained with 20 qubits and a depth of 2 (based on our Hypothesis) using a single node from the Fujitsu simulation cluster, the training time becomes too large and the cluster time outs.

3.4.3 Problems with 20 qubits on multiple nodes

When the pure quantum model is trained with 20 qubits and a depth of 2 (based on our hypothesis) using multiple nodes from the Fujitsu simulation cluster, the cluster deadlocks and disconnects.

4. AD drug discovery

Drug discovery [2] can be described as the process of identifying chemical entities that have the potential to become therapeutic agents. The key goal of drug discovery is the recognition of new molecular entities that may be of value in the treatment of diseases that qualify as presenting unmet medical needs.

Using an open source dataset from ChEMBL, a computational model is trained to generate the possible drug compounds which may slow down the progression. This model is trained to create newer drug structures targeting the disease.

4.1 Data preprocessing

The database is queried for single protein targets based on their positive bioactivity towards inhibiting this AChE inhibitor. The bioactivity data for Human Acetylcholinesterase which has a lower IC₅₀ value (active) has been selected for model training. The dataset contains 2608 molecules targeting AChE inhibition with each having 881 features.

4.2 Quantum circuit

We will use the Generative modeling approach using Quantum Computing to create newer molecules which can be the possible targets for Alzheimer's disease. The ChEMBL pre-processed dataset is again used here for training but the molecules which have an bioactivity towards the disease are being taken for training. We use the patch method for quantum GAN as mentioned in reference [22]. This method uses several quantum generators, with each sub generator responsible for constructing a small patch of the final molecular features. The training procedure is shown in the below Figure 8.

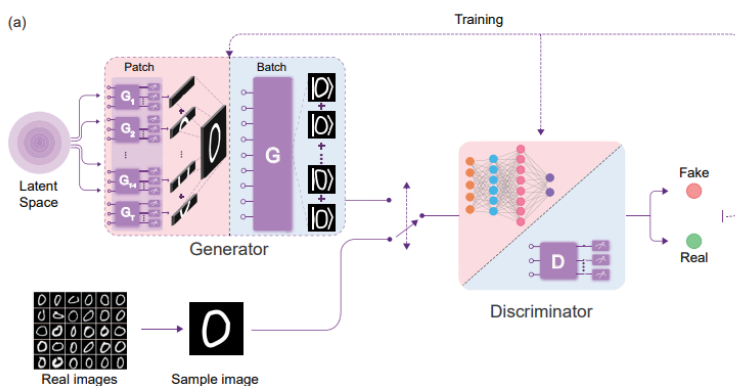


Figure 8 - Quantum GAN training

The training is being done using a generator and discriminator. The generator is the quantum model (along with the sub models) which creates the patches of the molecular features. The discriminator is a classical model which is being trained to predict whether the generated molecular features are real or fake. The generator quantum model uses the same 4 stages - initialization, transformation, trainable ansatz and measurement.

- *Initial State preparation* - All 0 states.
- *Transformation* - Angle Embedding (Y rotations).
- *Trainable Ansatz* - Ansatz [22] described in Figure 9.
- *Measurement* - Z measurement on all the qubits.

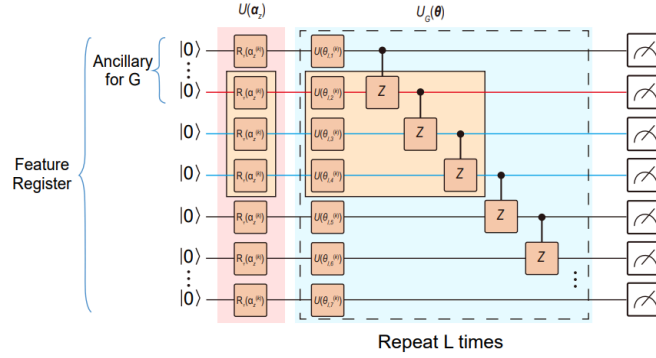


Figure 9 - Quantum GAN trainable ansatz

4.3 Simulator used

This is being coded with Python and using the mpiQulacs package provided by the Fujitsu environment. It is run on a Fujitsu cluster simulator as described in reference paper [21].

4.4 Results and challenges

4.4.1 Gradient estimation challenges

As was discussed in Section 3.4.1, the lack of gradient-based optimization in Qulacs [28] means we must rely on less effective Quasi-Newton methods.

4.4.2 Limitations with training

Using a 10 qubit quantum generator model, we require 80 different circuits being trained for generation and the outputs being evaluated by the discriminator quantum model which is also huge. This causes an overhead in the training time and times out the cluster. The discriminator model can also be created using classical deep neural networks, but the training required heavy memory and CUDA based GPU requirements.

By using a higher number of qubits, the training time for generation and discrimination can be significantly reduced. The main problem here is that, using multiple nodes from the Fujitsu simulation cluster for running the quantum circuit having 30 qubits causes a deadlock in the cluster and it disconnects.

5. Addressing evaluation criteria for the Fujitsu Quantum Simulator Challenge

5.1 Uniqueness of Solution

While we leveraged various input encoding techniques and parameterized quantum circuits in the literature, a great deal of thought went into applying these techniques to the applications explored in this project.

5.2 Solution Quality

Results in Section 2 – classifying structural MRI brain images into various stages of dementia – show that our hybrid classical-quantum ML model (97.57% accuracy) performs slightly better than a purely classical ML model (95.46% accuracy). Recall, this result was obtained in a Google Collaboratory (due in part to the availability of CUDA-based GPUs).

Results in Section 3 – drug identification for Alzheimer’s disease – showed an initial accuracy of 57.35% with 10 qubits on a single node of the Fujitsu quantum simulator. Accuracy with 20 qubits could not be demonstrated, as the 20 qubit simulation timed-out on a single node and deadlocked on multiple nodes.

In Section 4, drug discovery using quantum GANs, the training complexity could not be supported by a single node in the Fujitsu quantum simulator because of time-out. It could not be supported by multiple nodes due to deadlock.

5.3 Business Impact

- Value Proposition: Provide a Quantum Machine Learning powered diagnostic and drug discovery tool for dementia patients.
- Key Partnerships: Partner with pharmaceutical companies, hospitals, and imaging centers to implement our solutions back to industry.
- Key Activities: Integrate platform into hospitals' and imaging centers' IT systems for seamless workflow. Research new techniques to enhance model performance and application.
- Key Resources: Technical talent in quantum computing, quantum machine learning, neuroscience, and software engineering. Access to quantum computing infrastructure. De-identified datasets of past MRI scans.
- Channels: Sell directly to hospital networks, pharmaceutical and imaging clinics. Allow integration with their electronic medical records systems. Provide a platform via secure cloud services.
- Customer Segments: Radiology and imaging departments at hospitals and medical centers. Also pharmaceutical companies interested in drug discovery for Alzheimer's based on platform insights.
- Cost Structure: Development of quantum algorithms and ML models. Cloud computing and data storage fees. Software engineering team. Marketing and sales staff. Technical support for clients.
- Revenue Streams: SaaS-style recurring fees for access to cloud platform capabilities. Additional fee per scan analyzed. Pharma research and drug development partnerships.

5.4 Social impact

(SDG = Sustainable Development Goals)

- SDG 3 - Good Health and Well-Being: This project aims to improve early diagnosis and management of Alzheimer's disease, which directly contributes to promoting healthy lives and well-being. It addresses a major global health challenge.
- SDG 9 - Industry, Innovation and Infrastructure: The project involves developing and leveraging leading-edge technologies like quantum computing and machine learning. It promotes building innovation infrastructure and fostering new healthcare industry applications.
- SDG 17 - Partnerships for the Goals: The project requires cross-sector collaboration spanning healthcare, technology companies, academia, and government. These partnerships can enhance the research and maximize real-world impact.

The development of quantum machine learning techniques to detect Alzheimer's disease holds promise for significantly improving quality of life for patients and caregivers. By identifying symptoms sooner, patients can potentially get critical treatments when they are most effective at slowing cognitive decline. This enables them to maintain independence longer and continue engaging socially before dementia impacts their function. Early intervention can also reduce demands on family and friends providing care, lessening their risk of mental and physical health strains from the stresses of caregiving.

5.5 Scalability

The models proposed for this project are scalable and can be used directly for other applications involving classification or generative modeling. For example, with respect to the hybrid quantum-classical ML model in Section 2, the Resnet34 feature extractor along with the quantum classifier circuit can be used in a variety of image classification problems, such as histopathological cancer detection, brain tumor detection, and lung cancer detection. As another example, the quantum GAN of Section 4 can be used in a wide variety of generative modeling applications such as artistic image generation, music generation, etc.

5.6 Contribution to quantum emulator enhancement

In Sections 3 and 4, we highlighted problems with Qulacs (lack of gradient-based optimization of parameterized circuit parameters) and our difficulties exploiting multiple nodes in the Fujitsu simulation environment. We hope that our documentation of these problems will help with future competitions, such as deeper documentation of mpiQulacs as well as debug assistance.

References

1. Life after a dementia diagnosis and dementia life expectancy. Age Space. (n.d.). <https://www.agespace.org/dementia/life-expectancy>.
2. Edward A. Sausville, Chapter 30 - Drug Discovery, Editor(s): Arthur J. Atkinson, Shiew-Mei Huang, Juan J.L. Lertora, Sanford P. Markey, Principles of Clinical Pharmacology (Third Edition), Academic Press, 2012, Pages 507-515, ISBN 9780123854711.
3. Anusuya S, Keshewani M, Priya KV, Vimala A, Shanmugam G, Velmurugan D, Gromiha MM. Drug-Target Interactions: Prediction Methods and Applications. Curr Protein Pept Sci. 2018;19(6):537-561. doi: 10.2174/1389203718666161108091609. PMID: 27829350.
4. Dubey, S. (2019, December 26). Alzheimer's dataset (4 class of images). Kaggle. <https://www.kaggle.com/datasets/tourist55/alzheimers-dataset-4-class-of-images>
5. ChemBL Database. EMBL-EBI homepage. (n.d.). <https://www.ebi.ac.uk/chembl/>
6. Scientist, D. D. J. D., & Engineer, K. B. S. (2023, September 8). Machine learning mastery. MachineLearningMastery.com. <https://machinelearningmastery.com/>
7. He, K., Zhang, X., Ren, S., & Sun, J. (2015). Deep Residual Learning for Image Recognition. arXiv. <https://doi.org/https://doi.org/10.48550/arXiv.1512.03385>
8. PennyLane. PennyLane. (n.d.). <https://pennylane.ai/>
9. Mottonen, M., Vartiainen, J. J., Bergholm, V., & Salomaa, M. M. (2005). Transformation of quantum states using uniformly controlled rotations. Quantum Information and Computation, 5(6), 467–473. <https://doi.org/10.26421/qic5.6-5>.
10. Schuld, M., & Petruccione, F. (2019). Supervised learning with Quantum Computers. Springer.
11. Qiskit. (n.d.). <https://qiskit.org/>
12. McClean, J. R., Boixo, S., Smelyanskiy, V. N., Babbush, R., & Neven, H. (2018a). Barren Plateaus in quantum neural network training landscapes. Nature Communications, 9(1). <https://doi.org/10.1038/s41467-018-07090-4>
13. YouTube. (2022). QHack 2022: Marco Cerezo —Barren plateaus and overparametrization in quantum neural networks. YouTube. Retrieved October 6, 2023, from <https://www.youtube.com/watch?v=rErONNdHbjg>.
14. Cerezo, M., Sone, A., Volkoff, T., Cincio, L., & Coles, P. J. (2021). Cost function dependent barren plateaus in shallow parametrized quantum circuits. Nature Communications, 12(1). <https://doi.org/10.1038/s41467-021-21728-w>
15. Dataprofessor. (n.d.). Dataprofessor/bioinformatics_freecodecamp. GitHub. https://github.com/dataprofessor/bioinformatics_freecodecamp.git
16. Rdkit. (n.d.). Rdkit/rdkit: The official sources for the RDKit Library. GitHub. <https://github.com/rdkit/rdkit>
17. McGleenon BM, Dynan KB, Passmore AP. Acetylcholinesterase inhibitors in Alzheimer's disease. Br J Clin Pharmacol. 1999 Oct;48(4):471-80. doi: 10.1046/j.1365-2125.1999.00026.x. PMID: 10583015; PMCID: PMC2014378.

18. Dataprofessor. (n.d.-a). Dataprofessor/bioinformatics: Bioinformatics stuff. GitHub.
<https://github.com/dataprofessor/bioinformatics.git>
19. Kim , R. (2023). Implementing a Hybrid Quantum-Classical Neural Network by Utilizing a Variational Quantum Circuit for Detection of Dementia. arXiv. <https://doi.org/https://doi.org/10.48550/arXiv.2301.12505>
20. Majumdar, R., Baral , B., Bhagamiya , B., & Roy , T. D. (2023). Histopathological Cancer Detection Using Hybrid Quantum Computing. arXiv . <https://doi.org/https://doi.org/10.48550/arXiv.2302.04633>.
21. Imamura , S., Yamazaki, M., Honda, T., Kasagi, A., Tabuchi, A., Nakao, H., Fukumoto, N., & Nakashima, K. (2022). mpiQulacs: A Distributed Quantum Computer Simulator for A64FX-based Cluster Systems. arXiv. <https://doi.org/https://doi.org/10.48550/arXiv.2203.16044>
22. Huang, He-Liang, et al. "Experimental quantum generative adversarial networks for Image Generation." *Physical Review Applied*, vol. 16, no. 2, 27 Aug. 2021, <https://doi.org/10.1103/physrevapplied.16.024051>.
23. Wierichs, D., Izaac, J., Wang, C., & Lin, C. Y.-Y. (2022). General parameter-shift rules for quantum gradients. *Quantum*, 6, 677. <https://doi.org/10.22331/q-2022-03-30-677>.
24. Schuld, M., Bergholm, V., Gogolin, C., Izaac, J., & Killoran, N. (2019). Evaluating analytic gradients on quantum hardware. *Physical Review A*, 99(3). <https://doi.org/10.1103/physreva.99.032331>.
25. (1963, October 1). How does the L-BFGS work?. Cross Validated.
<https://stats.stackexchange.com/questions/284712/how-does-the-l-bfgs-work>
26. Sagingalieva A, Kordzanganeh M, Kenbayev N, Kosichkina D, Tomashuk T, Melnikov A. Hybrid Quantum Neural Network for Drug Response Prediction. *Cancers (Basel)*. 2023 May 10;15(10):2705. doi: 10.3390/cancers15102705. PMID: 37345042; PMCID: PMC10216276.
27. Batra K, Zorn KM, Foil DH, Minerali E, Gawriljuk VO, Lane TR, Ekins S. Quantum Machine Learning Algorithms for Drug Discovery Applications. *J Chem Inf Model*. 2021 Jun 28;61(6):2641-2647. doi: 10.1021/acs.jcim.1c00166. Epub 2021 May 25. PMID: 34032436; PMCID: PMC8254374.
28. Suzuki, Y., Kawase, Y., Masumura, Y., Hiraga, Y., Nakadai, M., Chen, J., Nakanishi, K. M., Mitarai, K., Imai, R., Tamiya, S., Yamamoto, T., Yan, T., Kawakubo, T., Nakagawa, Y. O., Ibe, Y., Zhang, Y., Yamashita, H., Yoshimura, H., Hayashi, A., & Fujii, K. (2021). Qulacs: A fast and versatile quantum circuit simulator for research purpose. *Quantum*, 5, 559. <https://doi.org/10.22331/q-2021-10-06-559>
29. Pytorch. PyTorch. (n.d.). <https://pytorch.org/>
30. Mullen, S. (2022, March 1). An introduction to lean canvas. Medium.
https://medium.com/@steve_mullen/an-introduction-to-lean-canvas-5c17c469d3e0